



**HAL**  
open science

## **A bilayered PVA/PLGA-bioresorbable shuttle to improve the implantation of flexible neural probes**

Jolien Pas, Alexandra L Rutz, Pascale P. Quilichini, Andrea Slézia, Antoine Ghestem, Attila Kaszas, Mary J Donahue, Vincenzo F Curto, Rodney P O'connor, Christophe Bernard, et al.

### ► To cite this version:

Jolien Pas, Alexandra L Rutz, Pascale P. Quilichini, Andrea Slézia, Antoine Ghestem, et al.. A bilayered PVA/PLGA-bioresorbable shuttle to improve the implantation of flexible neural probes. Journal of Neural Engineering, 2018, 15, 10.1088/1741-2552/aadc1d . hal-03582767

**HAL Id: hal-03582767**

**<https://amu.hal.science/hal-03582767>**

Submitted on 21 Feb 2022

**HAL** is a multi-disciplinary open access archive for the deposit and dissemination of scientific research documents, whether they are published or not. The documents may come from teaching and research institutions in France or abroad, or from public or private research centers.

L'archive ouverte pluridisciplinaire **HAL**, est destinée au dépôt et à la diffusion de documents scientifiques de niveau recherche, publiés ou non, émanant des établissements d'enseignement et de recherche français ou étrangers, des laboratoires publics ou privés.



Distributed under a Creative Commons Attribution 4.0 International License

PAPER • OPEN ACCESS

## A bilayered PVA/PLGA-bioresorbable shuttle to improve the implantation of flexible neural probes

To cite this article: Jolien Pas *et al* 2018 *J. Neural Eng.* **15** 065001

View the [article online](#) for updates and enhancements.



**IOP | ebooks™**

Bringing you innovative digital publishing with leading voices to create your essential collection of books in STEM research.

Start exploring the collection - download the first chapter of every title for free.

# A bilayered PVA/PLGA-bioresorbable shuttle to improve the implantation of flexible neural probes

Jolien Pas<sup>1,2</sup>, Alexandra L Rutz<sup>1,4</sup>, Pascale P Quilichini<sup>3</sup>, Andrea Slézia<sup>3</sup>, Antoine Ghestem<sup>3</sup>, Attila Kaszas<sup>3,5</sup>, Mary J Donahue<sup>1</sup>, Vincenzo F Curto<sup>1,4</sup>, Rodney P O'Connor<sup>1</sup>, Christophe Bernard<sup>3</sup>, Adam Williamson<sup>3</sup> and George G Malliaras<sup>1,4</sup>

<sup>1</sup> Department of Bioelectronics, Mines Saint-Etienne, Center of Microelectronics in Provence, F-13541 Gardanne, France

<sup>2</sup> Panaxium SAS, 67 Cours Mirabeau, 13100 Aix-en-Provence, France

<sup>3</sup> Aix Marseille Univ, INSERM, INS, Inst Neurosci Syst, 13005 Marseille, France

<sup>4</sup> Electrical Engineering Division, Department of Engineering, University of Cambridge,

9 JJ Thomson Ave, Cambridge CB3 0FA, United Kingdom

<sup>5</sup> Aix-Marseille Univ, CNRS UMR 7289, Inst de Neurosci de la Timone, 13005 Marseille, France

E-mail: [gm603@cam.ac.uk](mailto:gm603@cam.ac.uk)

Received 19 April 2018, revised 21 August 2018

Accepted for publication 22 August 2018

Published 11 September 2018



CrossMark

## Abstract

*Objective.* Neural electrophysiology is often conducted with traditional, rigid depth probes. The mechanical mismatch between these probes and soft brain tissue is unfavorable for tissue interfacing. Making probes compliant can improve biocompatibility, but as a consequence, they become more difficult to insert into the brain. Therefore, new methods for inserting compliant neural probes must be developed. *Approach.* Here, we present a new bioresorbable shuttle based on the hydrolytically degradable poly(vinyl alcohol) (PVA) and poly(lactic-co-glycolic acid) (PLGA). We show how to fabricate the PVA/PLGA shuttles on flexible and thin parylene probes. The method consists of PDMS molding used to fabricate a PVA shuttle aligned with the probe and to also impart a sharp tip necessary for piercing brain tissue. The PVA shuttle is then dip-coated with PLGA to create a bi-layered shuttle. *Main results.* While single layered PVA shuttles are able to penetrate agarose brain models, only limited depths were achieved and repositioning was not possible due to the fast degradation. We demonstrate that a bilayered approach incorporating a slower dissolving PLGA layer prolongs degradation and enables facile insertion for at least several millimeters depth. Impedances of electrodes before and after shuttle preparation were characterized and showed that careful deposition of PLGA is required to maintain low impedance. Facilitated by the shuttles, compliant parylene probes were also successfully implanted into anaesthetized mice and enabled the recording of high quality local field potentials. *Significance.* This work thereby presents a solution towards addressing a key challenge of implanting compliant neural probes using a two polymer system. PVA and PLGA are polymers with properties ideal for translation: commercially available, biocompatible with FDA-approved uses and bioresorbable. By presenting new ways to implant compliant neural probes, we can begin to fully evaluate their chronic biocompatibility and performance compared to traditional, rigid electronics.



Original content from this work may be used under the terms of the [Creative Commons Attribution 3.0 licence](https://creativecommons.org/licenses/by/3.0/). Any further distribution of this work must maintain attribution to the author(s) and the title of the work, journal citation and DOI.

Keywords: bioelectronics, neural depth probes, poly vinyl alcohol (PVA), poly(lactic-co-glycolic acid) (PLGA), electrophysiology

 Supplementary material for this article is available [online](#)

## Introduction

Neural depth probes are neural interfaces designed to record neural activities and are used to help researchers understand the complex electrochemical mechanisms inside the brain. Many researchers require long-term, stable recordings, yet irreversible brain damage and complete loss of recording function are unpreventable consequences when using traditional depth probes [1, 2]. These traditional depth probes are made of silicon or metal, which are rigid materials that have elastic moduli above 100 GPa [1, 2]. In contrast, the brain is a very soft tissue with a modulus ranging from 0.1 to 10 kPa [2, 3]. Mechanical mismatch as large as 7 orders of magnitude leads to irreversible tissue damage and eventual electrode failure in months to at most a couple of years after implantation due to the glial response [3, 4].

To improve the long-term function of depth probes, more compliant probes have been investigated with promising results [4]. Compliant probes are either made of softer materials and/or by making the materials significantly thinner. Examples include polymers, such as polyimide [5, 6], parylene-C [7–9] and polydimethylsiloxane (PDMS) [10], hydrogels [11, 12], carbon nanotubes [13, 14], graphene [15] and silicon nanomembranes [16, 17]. However, the use of more compliant materials results in a more complicated surgical insertion of the depth probe [4]. Most flexible probes are unable to penetrate the brain without buckling and a temporary insertion system is necessary to place the probe at the desired location inside the brain. Solutions to tackle this include the use of a stiff shuttle which is removed after implantation (needle, wire, silicon shank) [18–20], the use of a microfluidic system which guides and physically assists the probe into the brain [21], and the use of a stiff shuttle that is not removed but loses its rigidity, dissolves or degrades inside the brain with time [22–30]. Due to the tissue trauma caused when implanting and retreating needles, wires or silicon shanks, we focused our work on bioresorbable polymer shuttles. Such shuttles do not require any surgical removal as they are broken down and excreted or resorbed in the body [31, 32]. Thus, at the end the flexible probe is left behind while the mechanically stiff shuttle diminishes on its own, which is a very promising solution to improve the long-term function of neural interfaces.

Various bioresorbable polymers have been reported to facilitate insertion of flexible depth probes into the brain [4]. The polymer polyethylene glycol (PEG) initially showed sufficient stiffness and fast degradation rates for this application [22, 23]. Another promising material is silk because of the suitable mechanical stiffness for brain penetration, potentially enabling fabrication of smaller devices which

consequently induce less brain damage [23]. Yet, the slow degradation and uninvestigated long-term biocompatibility of silk are concerning drawbacks [33]. Other natural polymers have also been shown to successfully penetrate brain tissue (like cellulose and maltose [24, 25, 30] or gelatin [26]), but the properties of these polymers cannot be as easily tuned as synthetic polymers. From the synthetic polymers investigated for this application, tyrosine-derived polycarbonate showed great results [28, 29, 34]. This polymer is initially stiff and degrades within 2 h after implantation. However, the polymer is not commercially available as it is synthesized in-lab. Other options should therefore be investigated to find an easier solution to insert a flexible neural probe.

In this work, we focused on utilizing synthetic and commercially available polymers for the fabrication of biodegradable neural probe shuttles. Here, we provide a bi-layered solution to facilitate the penetration of a flexible parylene probe into the brain using two distinct bioresorbable polymers, poly(vinyl alcohol) (PVA) and poly(lactic-co-glycolic acid) (PLGA). Besides the benefit of being commercially available with many different properties (molecular weight, polymer ratio, etc...), PVA and PLGA are both used in FDA approved applications [35–40], making them even more attractive for this work. In brief, we report on the fabrication of the PVA/PLGA-shuttled parylene probes, the mechanical and electrical characterization of these probes, as well as their implantation *in toto* and *in vivo*, resulting in successful acute neural recordings.

## Materials and methods

### Probe fabrication

The fabrication process of our flexible probes includes the deposition and patterning of parylene-C (for simplicity, from now on named ‘parylene’), chromium, gold and PEDOT:PSS films, as previously reported [9]. Briefly, parylene was deposited on a glass wafer with an approximate thickness of 2  $\mu\text{m}$  using an SCS Labcoater 2. Two layers of photoresist, LOR (MicroChemicals) and S1813 (Shipley), were spin-coated on the parylene film. LOR was spun at 3000 rpm for 40 s and baked at 200 °C for 1 min. S1813 was spun at 5000 rpm for 40 s and baked at 115 °C for 2 min. The layers were exposed to UV-light (96  $\text{mJ cm}^{-2}$ ) using an SUSS MJB4 contact aligner and developed using MF 26 developer. The wafer was plasma treated for 1 min at 100 W with  $\text{O}_2$  using a reactive ion etcher (Oxford 80 plus plasma etcher). Then, a thin layer of 10 nm of chromium was deposited in a metal evaporator (Alliance Concept EVA450) to improve the adhesion of gold, which

was deposited next with a final thickness of 100 nm. Lift-off was performed leaving the wafer overnight in NMP (Sigma-Aldrich). Two layers of parylene were subsequently deposited, one as insulation layer and one as sacrificial layer during a later peel-off technique. A layer of 2% soap was added in between. The insulation layer was patterned with the probe outline, using AZ9260 spun at 3000 rpm for 40 s, baked at 110 °C for 2 min, exposed (65–90 mJ.cm<sup>-2</sup>), developed in AZ developer for 4 min and etched for 8 min at 400 W with 50 sccm O<sub>2</sub> and 5 sccm CHF<sub>3</sub>. The same was done after the sacrificial parylene layer was added to etch away the parylene at the microelectrode sites. Next, the PEDOT:PSS solution was prepared adding 5% (v/v) of ethylene glycol, 0.5 μl ml<sup>-1</sup> of dodecyl benzene sulfonic acid (DBSA) and 1 wt% of 3-glycidoxypropyltrimethoxy-silane (GOPS) to the aqueous dispersion (PH 1000 from H.C. Stark). This PEDOT:PSS solution was spin-coated twice, once at 3000 rpm and once at 1500 rpm. A baking of 1 min was done in between both steps at 90 °C. The sacrificial parylene layer was peeled-off and the films were baked at 140 °C for 1 h. Before the packaging, the probes were immersed in deionized water to remove any excess low molecular weight compounds inside the PEDOT:PSS film. Finally, the probes were removed from the wafer and zero insertion force (ZIF) cables (Mouser Electronics) were attached with anisotropic conductive film (ACF) using an APR-5000-DZ soldering machine. The fabricated flexible parylene probes were designed with an insertion tip of 3 mm long and 180 μm wide, containing six microelectrodes, each with an active area of 14 μm in diameter, and located at 90 μm distance from each other (center-to-center).

#### *Bioresorbable PVA/PLGA shuttle fabrication*

The fabrication of PVA/PLGA shuttles was performed on the backside of the flexible parylene probes. First, PDMS molds were made using epoxy-based negative photoresist SU8. SU8 2075 (Microchemicals) was deposited on a cleaned glass wafer and spun at 500 rpm for 10 s and 1000 rpm for 30 s for a final SU8 thickness of ~200 μm. Next, a soft bake at 65 °C and 95 °C for 7 and 45 min was performed, followed by UV exposure (SUSS MJB4 contact aligner, including an i-line filter, 350 mJ cm<sup>-2</sup>) and a post exposure bake of 5 and 15 min. After development in SU8 developer (Microchemicals) for 17 min, the glass wafer was wrapped in aluminum to form a dish and PDMS (1:10 of base:curing agent, Sigma-Aldrich) was deposited and cured in the oven at 70 °C overnight. The PDMS layer was then gently peeled-off from the wafer and the molds were ready for use. The next step was the alignment of a parylene probe into a PDMS mold. The probe with attached ZIF cable was placed into the mold with the electrode sites downwards. The mold was 100 μm wider than the actual probe to facilitate the alignment, which means that the width of the shuttle is 380 μm while the length remained the same. PVA (Sigma Aldrich, CAS number: 26780-50-7; 10000 g mol<sup>-1</sup>) was dissolved at 20 w/v in water by heating up the mixture for at least 1 h at 90 °C. The dissolved PVA was drop-casted onto the backside of the probe inside the mold and subsequently blade coated.

This complex was left in the oven for 15 min at 70 °C to slowly evaporate the water. A second PVA coating was done and again left in the oven for another 30 min. Next, the probe with PVA shuttle were removed from the mold with tweezers. To coat the tip with PLGA, the backside of the probe (i.e. the opposite side of the electrode side) was dipped into a 25 wv% PLGA (Sigma aldrich, CAS number: 9002-89-5; with a lactide:glycolide ratio of 65:35) acetone solution, unless mentioned otherwise. For the coating procedure, a small microtube (Sigma Aldrich, 1 ml) containing the PLGA solution was tilted to approximately 50° to bring the solution to the walls of the tube. With the probe held with tweezers, the probe was manually lowered onto the solution on the side walls of the microtube. After 5 s in contact with the solution, the probe tip was lifted and removed from the microtube. The acetone solvent evaporated fast at room temperature (RT) and the PVA/PLGA-shuttled parylene probe was ready for use.

#### *PVA/PLGA-shuttled probe characterization*

The thicknesses of PVA-shuttled probes and PVA/PLGA-shuttled probes were estimated using scanning electron microscopy (SEM) images and ImageJ. The thicknesses were calculated by taking into account the tilt of the imaged probes. The average thicknesses of PVA-shuttled probes and PVA/PLGA-shuttled probes were 82 ± 9 μm (*n* = 5) and 88 ± 8 μm (*n* = 3), respectively. Since PLGA is a slow degradable polymer, the amount of PLGA that would be present in the brain was evaluated by measuring the added weight on PVA shuttles after PLGA coating (Denver Instrument balance). The average PLGA mass on the tip was estimated at 17.5 ± 8.9 μg (*n* = 10).

#### *Dissolution testing*

The speed of dissolution was evaluated by dissolving PVA shuttles and PVA/PLGA shuttles in artificial cerebrospinal fluid (ACSF). Probe tips were first fixed at the base of the tip inside a 12 well-plate (Falcon™) using kapton tape. The well-plate was then fixed inside the microscope holder and the temperature inside the microscope chamber was set at 37 °C. In the meantime, ACSF was filtered through a 0.8 μm polytetrafluoroethylene (PTFE) filter and warmed up to 37 °C in a water bath before deposition. The dissolution of the shuttles was video recorded with a Zeiss microscope (Zeiss Axio Observer Z1). The time of dissolution started at the moment the tip was completely immersed in 1 ml ACSF and the video recording continued until the shuttle had been dissolved or until the first 3 min of immersion. The probe tips, which had not dissolved by that time, were kept immersed in ACSF and were stored in an incubator at 37 °C. Additional pictures were taken to evaluate any change in physical appearance in time due to further dissolution.

Note that besides PVA/PLGA-shuttled probes, also stand-alone PVA and PVA/PLGA shuttles were fabricated for characterization (i.e. without the inclusion of valuable parylene probes). These shuttles were fabricated as mentioned

before, yet without the initial alignment of parylene probes before polymer deposition. Since PVA would be exposed more without the inclusion of the parylene probe from one side, these shuttles were completely immersed in the PLGA solution (i.e. both front- and backside), unlike previously mentioned.

### Insertion testing

Agarose gels were used as brain model to first evaluate the mechanical strength of PVA and PVA/PLGA shuttles. Agarose gels were prepared at 0.6% w/w agarose in water and autoclaved at 121 °C for 20 min in 24 well-plates (Falcon™). The agarose gels were used as brain models and were kept wet with a few drops of water while stored in the fridge at 4 °C. During penetration tests, a microscope (Zeiss Axio Observer Z1) was used to visualize and record the horizontal penetration of the PVA/PLGA shuttles into the agarose models. Moreover, Coomassie blue was added to the solution of PVA during fabrication to improve the visualization of shuttle penetration. The shuttles were mounted onto a micromanipulator stage and manually inserted at the estimated speed of 0.3 mm s<sup>-1</sup>. Before continuing with *in vivo* experiments, the mechanical strength of the PVA/PLGA shuttled probes was also evaluated during insertion tests in extracted brain tissue (the reader is referred to the supplementary information, supporting video 5 ([stacks.iop.org/JNE/15/065001/mmedia](https://stacks.iop.org/JNE/15/065001/mmedia))).

### Electrical characterization

Impedance measurements were performed with a potentiostat (Autolab PGSTAT128N) in a three electrode configuration. The reference, counter and working electrode were a Ag/AgCl electrode, a Pt electrode and the depth probe, respectively. The characterization was done with probes that were fully coated (i.e. both front side and back side of the probes) with PLGA. The change in electrode impedance is investigated during for four weeks to study the influence of polymer degradation on electrode impedance. Measurements were performed in Dulbecco phosphate-buffered saline (DPBS) by applying a 10 mV root mean square sine wave with frequencies varied logarithmically from 1 Hz to 100 kHz. The average impedances are presented as mean ± SD.

### Mouse surgery

All experiments were conducted in accordance with Aix-Marseille Université and Inserm Institutional Animal Care and Use Committee guidelines. The protocol was approved by the French Ministry of National Education, Superior Teaching, and Research, approval number 01451-02. All surgical procedures were performed under anesthesia and every effort was made to minimize suffering.

Adult male C57 ( $n = 5$ ) mice were used for the *in vivo* experiments. Mice were housed in a 12h light/dark cycle with food and water available *ad libitum*. Mice were initially anesthetized with an intraperitoneal injection of a mixture of ketamine/

xylazine (ketamine, 100 mg kg<sup>-1</sup>; xylazine, 10 mg kg<sup>-1</sup>) and additional doses were given if needed. Mice were head-fixed in a stereotaxic frame (Kopf). After a subcutaneous injection of ropivacaine, a craniotomy was made (from bregma) 1.0 mm anteroposterior and 1.2 mm mediolateral. The dura mater was removed, and PVA/PLGA-shuttled probes were lowered into the cortex between 1.8 to 2.8 mm from the brain surface reaching the deep layers of the cortex or the hippocampus. Up to 4 probes were tested per animal to be in line with the 3R's rule of animal ethics. When using multiple probes, a different insertion point at the surface of the cortex was chosen for each probe. The exact speed of insertion was not measured, however based on the insertion time and the depth which were reached, the estimated speed of insertion is 0.2 mm s<sup>-1</sup>.

### Acute recordings

Extracellular signals were amplified (1000×), bandpass filtered (0.1 Hz or 1 Hz to 5 kHz) and acquired continuously at 32 kHz with a Digital Lynx system (NeuraLynx). Raw data were preprocessed using NEUROSUITE [40] and the signals were downsampled to 1250 Hz for the local field potential (LFP) analysis, which was performed using custom-written MATLAB (MathWorks) scripts.

### LFP signal analysis

To estimate the baseline quality of the LFP measurements, the Root Mean Square (RMS, with the MATLAB built-in RMS function) value of short epochs of baseline were computed during the less excitable and low network activity state ('Down State') of the anesthesia-induced slow oscillations [41]. The Down State epochs were visually identified as moments of flat baseline and tagged in the Neuroscope software. Epochs of 10–50 ms were tagged approximately every second (the slow oscillations having a ~1 Hz frequency) for 3 min, from the moment the parylene probe reached its final position in the brain.

Power spectra of short LFP periods (4 s) were performed on pre-whitened LFPs and computed between 0.1 and 1000 Hz using a modified version of the multi-taper FFT MATLAB package by Mitra and Pesaran [42]: FFT window size of 1 s, three to five tapers, frequency bins = 0.15 Hz, no overlap between successive windows, time bandwidth = 3 [42, 43].

### Histology and immunocytochemistry

After the acute recordings, the mice were injected with a lethal dose of pentobarbital Na (150 mg kg<sup>-1</sup>, i.p.) and perfused intracardially with 4% paraformaldehyde solution in 0.1 M phosphate buffer (PB), pH 7.4. The brains were removed and post-fixed at 4 °C overnight. They were then rinsed in PB and sliced into 40 μm or 60 μm thick coronal sections by a Vibratome (Leica). The position of the electrodes was confirmed histologically on Cresyl Violet Nissl stained sections (NeuroTrace 500/525 Green Fluorescent Nissl Stain, Thermofisher).

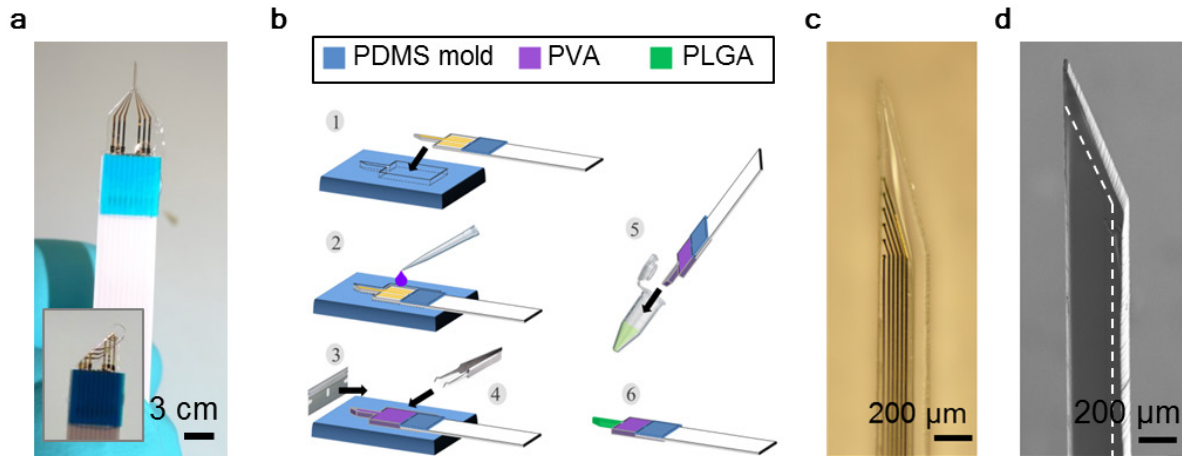


**Figure 1.** Fabrication of probes. (a) Photograph of a parylene-C probe which is held up and stiffened with a bioresorbable PVA-PLGA shuttle. Inset: a flexible probe without the bioresorbable shuttle that curls upon removal for fabrication substrate. (b) Schematic of the fabrication process of the bioresorbable shuttle. (*Step 1*) Alignment of ZIF-attached probe in PDMS mold. (*Step 2*) Deposition of a 20 w/v PVA/water solution. (*Step 3*) Blade-casting the PVA solution. (*Step 4*) Removal of probe from the mold after an oven treatment of 45 min. (*Step 5*) Dip-coating the PVA-shuttled probe into a 25 wt% PLGA (65:35) acetone solution. (*Step 6*) Fast evaporation of the acetone from the tip, which results in a PVA/PLGA-shuttled probe. (c) A phase contrast image and (d) SEM image of a PVA/PLGA-shuttled probe. The white dash lines show the boundary of the parylene probe within the bioresorbable polymer shuttle.

## Results and discussion

Our flexible depth probes were made of parylene, containing metal microelectrodes coated with conducting polymer poly(3,4-ethylenedioxythio-phenylene):poly(styrene-sulfonate) (PEDOT:PSS). The probe fabrication was reported earlier [9]. Briefly, it involves the patterning of parylene, gold and PEDOT:PSS via photolithography and parylene peel-off. The microelectrodes are coated with PEDOT:PSS to lower the impedance and obtain a better signal-to-noise ratio during *in vivo* recordings [44, 45].

The bioresorbable PVA/PLGA shuttle was then fabricated on the backside of the probe to rigidify the overall flexible device. Before polymer deposition, a ZIF cable was first attached to the parylene probe as temperatures above the melting temperatures of the polymers are applied during attachment of the cable. Without the bioresorbable polymer support, the parylene probe curled and was difficult to handle being only 4  $\mu\text{m}$  thin (Inset, figure 1(a)). The main function of the polymer coating was to add rigidity to the probe, which kept the probe straight as illustrated in figure 1(a). In order to apply the polymer coating, the probe was first aligned into a PDMS mold with the microelectrodes facing the mold (figure 1(b), *Step 1*). Then, a 20 w/v PVA solution was deposited on the back-side of the probe followed by blade-casting (figure 1(b), *Step 2–3*). The device was subsequently placed in the oven with the mold for at least 15 min to homogeneously remove the solvent from the polymer solution. A second deposition was performed and again dried in the oven for another 30 min. This protocol is thereby different from prior molding work [23, 29], during which the bioresorbable polymers were dried under ambient conditions. The latter process is time consuming and, in our environmental conditions, resulted in curled tips. In contrast, the oven procedure resulted in straight tips. Once the PVA was dry, the probe was taken up with tweezers (*Step 4*) and dipped with the backside of the probe into a

25 wt% PLGA (65:35) acetone solution (*Step 5*). The acetone quickly evaporates (*Step 6*) and the final result is a bi-layered PVA/PLGA-shuttled probe with a width of 380  $\mu\text{m}$  (figure 1(c)). A sharp tip was achieved and the probes were of an average thickness of  $88 \pm 8 \mu\text{m}$  ( $n = 3$ ) (figure 1(d)).

The use of two different bioresorbable polymers as shuttle material was necessary to enable insertion of flexible depth probes into a wet brain. This was evaluated with dissolution experiments of the probe tips immersed in ACSF at 37 °C and with insertion testing using a 0.6% agarose brain model and complete hippocampal tissues for penetration. As shown in figure 2(a), the PVA shuttle completely dissolved within 30 s after immersion, thereby losing rigidity (supporting video 1). With the addition of PLGA, the dissolution of the PVA polymer was slowed down (figure 2(b)). Unlike PVA and other hydrolytically degrading polymers, PLGA degrades slowly through bulk erosion as shown both *in vitro* and *in vivo* [36, 46]. This degradation type is not as common as surface erosion under hydrolytically degradable polymers [47]. It's what makes PLGA so attractive for this application: it does not immediately dissolve when in contact with a wet surrounding. The polymer is mentioned as the most investigated biodegradable polymers [31]. It showed tunable biodegradable properties and excellent biocompatible characteristics which resulted in multiple FDA approved medical uses, like in sutures, drug delivery devices and tissue engineering [31, 40]. In this work, the addition of a thin layer of PLGA (estimated at 6  $\mu\text{m}$  using SEM) resulted in a delayed interaction of water with PVA and slows down shuttle dissolution. We believe that once water permeates through the PLGA layer, PVA starts to dissolve slowly and diffuses out of the PLGA layer. The PLGA layer remains nevertheless intact, at least for more than a month in ACSF at 37 °C (supplementary figure 1). Along with the dissolution of PVA from the shuttle, we observed that the parylene probe became compliant again after several minutes of immersion (supporting video 2).

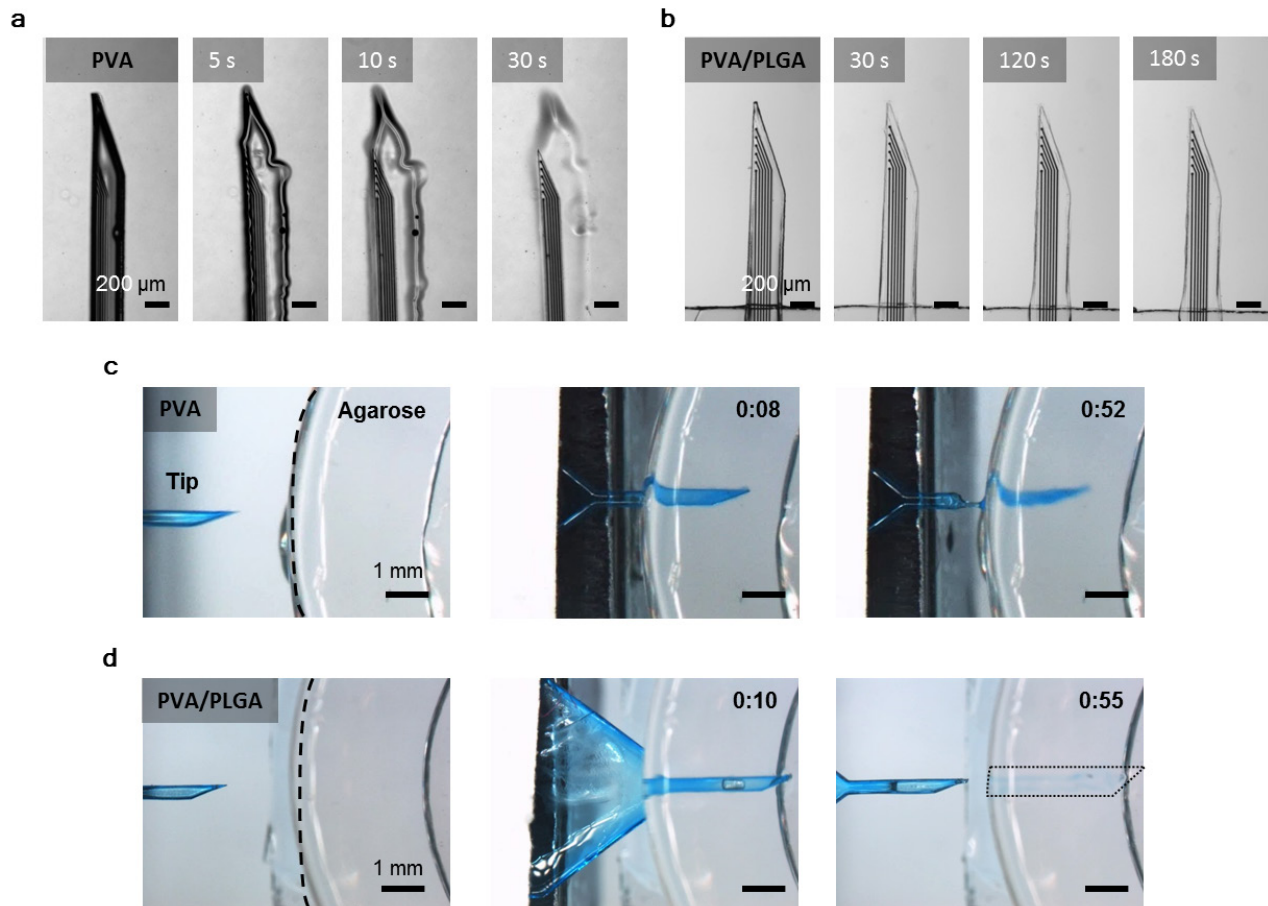


**Figure 2.** Dissolution and insertion characteristics of probes. (a) Snapshots of the dissolution of a PVA-shuttle at different times during immersion of the tip in ACSF at 37 °C. The PVA shuttle starts dissolving within 5 s. The diffuse borders indicate dissolving polymer. The shuttle is almost completely dissolved after 30 s. (b) Snapshots of the immersion of a PVA/PLGA-shuttled probe tip in ACSF at 37 °C. The PLGA/PVA shuttle does not seem to change in time, unlike the PVA shuttle. No visible dissolution is observed and the tip remains intact for more than 3 min. (c) Microscope images showing the penetration of a PVA shuttle tip into a wet agarose brain model. A blue dye was added to the PVA solution before fabrication of the shuttle to better visualize the penetration. The boundary of the brain model is indicated with a black dashed line and the times after penetration are indicated in the upper right corners. The PVA shuttle clearly penetrated the brain model with an estimated penetration speed of  $0.3 \text{ mm s}^{-1}$ . The dissolution of the PVA started nevertheless immediately when placed in contact with the wet brain model. Almost 1 min after the placement of the PVA shuttle inside the brain, the tip was dissolved and thus not well connected anymore to the part which was not in contact with the wet brain. (d) Microscope images showing the penetration of a PVA/PLGA shuttle into the wet brain model at the same penetration speed of  $0.3 \text{ mm s}^{-1}$ . During penetration, an air bubble got trapped in between the agarose and shuttle. This occasionally happened, but it did not seem to affect the penetration. Unlike PVA shuttles, the tip of the PVA/PLGA shuttle could be completely retreated. The tip seemed slightly less blue and blue residue was seen within the agarose brain model (encircled with black dashed lines). This shows the partial dissolution of PVA, which diffused out of the PLGA layer during penetration.

Although the PVA shuttles showed sufficient stiffness to penetrate the brain model, the fast dissolution made it difficult to place the probe at its desired depth before dissolution (figure 2(c) and supporting video 3). PVA shuttles were colored blue during the insertion tests by the addition of a dye to improve the visualization of the probe penetration. Since PVA shuttles started dissolving within 5 s when placed in contact with an aqueous solution (figure 2(a)), brain insertion was no longer possible. In contrast, the PVA/PLGA shuttle was easily inserted into the brain model (figure 2(d)). The blue color inside the agarose model after retracting the shuttle clearly showed that some PVA had already dissolved during this first penetration. Besides slowing down the dissolution of PVA, the additional benefit of adding PLGA was that it enabled multiple brain penetrations with the same probe

(supporting video 4). Repositioning of depth probes inside the brain was sometimes needed to reposition the probe if the initial location was not close enough to firing neurons. This again shows the great benefit of PLGA, not only does it delay the dissolution with the addition of approximately  $18 \mu\text{g}$  of PLGA on the tip, it maintains also the necessary rigidity of the shuttle to penetrate a brain multiple times. Finally, probe penetration has also been confirmed in complete hippocampal preparations (supporting video 5).

The difference in degradation speeds with this bi-layered polymer shuttle could especially be beneficial for future additions of anti-inflammatory drugs to improve the biocompatibility of implanted neural probes. PVA and PLGA have been used for fast (seconds) [37, 39] and slow [48, 49] drug delivery, respectively, and offer opportunities for tunable

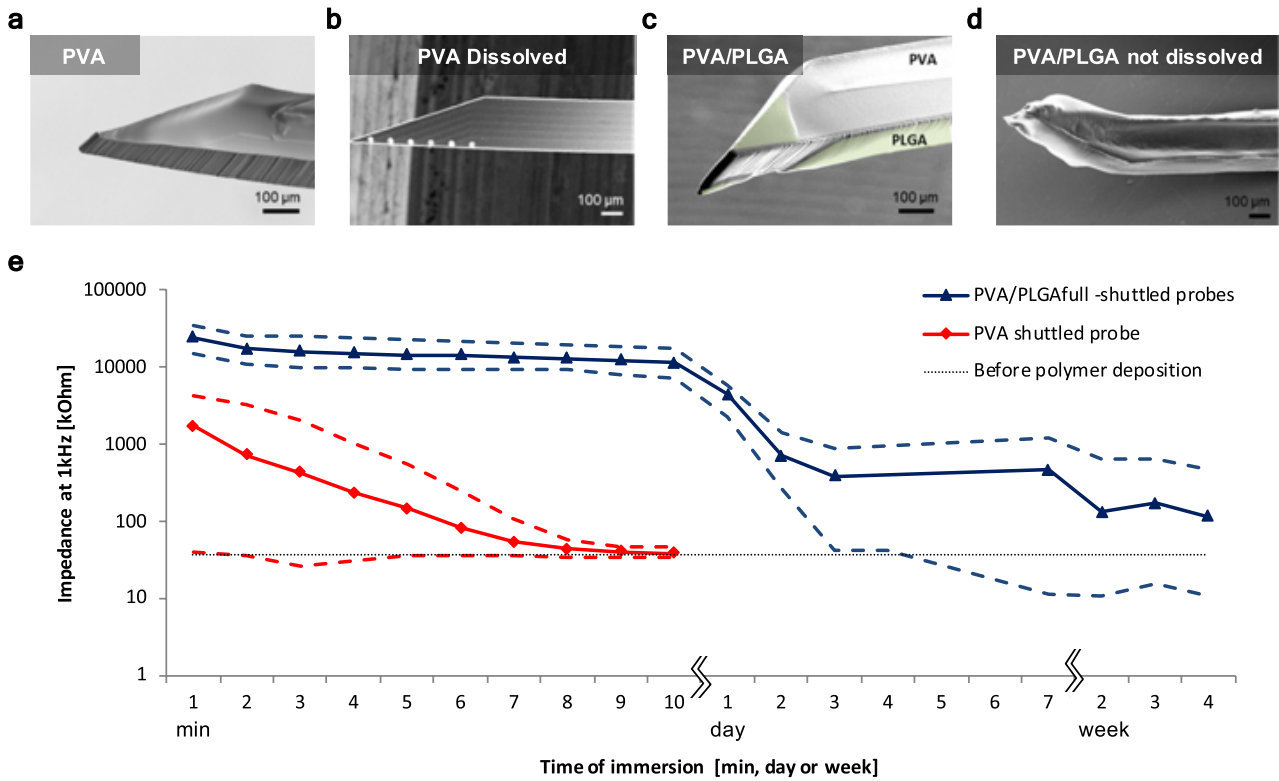


**Figure 3.** Electrical characterization of probes. (a)–(d) SEM pictures of (a) a PVA-shuttled probe, (b) a clean probe after 10 min immersion of the PVA-shuttled probe in saline, (c) a PVA/PLGA-shuttled probe and (d) the same PVA/PLGA-shuttled probe still covered in polymer after 10 min of immersion in saline. Note that the PVA/PLGA shuttled probes for electrical characterization are fully coated with PLGA, i.e. both front- and backside of the probe, to study the influence of polymer degradation on electrode impedance. While PVA quickly dissolves and leaves behind a clean probe, PVA/PLGA remains present on the probe and the microelectrodes 10 min after immersion. (e) The average impedances of the investigated electrodes before polymer deposition are illustrated with straight lines (red, PVA batch; blue, PVA-PLGA batch). The change in average impedance at 1 kHz as function of time during the immersion of PVA and PVA/PLGA shuttled probes in saline is shown by the red and blue curves, respectively. The dashed lines below and above the average impedance represent the minimum and maximum values of the measured values. Between the daily measurements, the probes were incubated at 37 °C in saline. A fast change in electrode impedance is observed for PVA shuttled probes, with the restoration of its original (i.e. before PVA deposition) low impedance after 10 min of immersion ( $n = 5$  electrodes) when the PVA is dissolved. The addition of PLGA on both the front- and backside of the PVA-shuttled probes prevents the fast dissolution, yet also significantly slows down the restoration of the low impedances of the electrodes (min 1–10:  $n = 4$  electrodes; day 1–7:  $n = 12$  electrodes; week 2–4:  $n = 10$  electrodes). This is explained by the coverage of PVA/PLGA on the microelectrodes. A decreasing trend is nevertheless observed. While only a few electrodes (3 out of 12,  $n = 12$ ) showed impedances below a 100 kΩ after a week, more electrodes (6 out of 10,  $n = 10$ ) dropped back to this lower value after four weeks in saline.

release profiles from hours to months [36, 49] to tackle both acute and chronic inflammation.

Before evaluating the electrical characteristics of the PVA/PLGA shuttled probes, the presence of the polymers on top of the electrodes was investigated using scanning electron microscopy (SEM). Despite all care taken and placing the probe upside down in the mold during deposition of PVA, the microelectrodes of the probes were inevitably covered by a thin layer of polymer (figure 3(a)). The outline of the probe within the shuttle was visible, yet covered with polymer. Nevertheless, immersion of the PVA-shuttled probes into a saline solution for 10 min caused complete dissolution of the shuttle, leaving behind a clean parylene probe (figure 3(b)). Also, the addition of PLGA to the PVA-shuttled probes occasionally covered a part of the front side of the probe (figure 3(c), with PLGA colored in green), despite efforts to dip-coat solely the backside of the probe tip. To investigate the effect on the presence of PLGA when covering the electrodes, a PVA-shuttled probe was fully coated with PLGA, i.e. covering both

front- and backside of the probe. When placing this probe into a saline solution for 10 min, it remained completely covered with polymer (figure 3(d)).

Manually dip-coating the backside of the micrometer scaled probe with PLGA remained challenging, yet the variability in thickness of the coating remained small. While PVA-shuttled probes were of a thickness of  $82 \pm 9 \mu\text{m}$  ( $n = 5$ ), PVA/PLGA shuttled probes showed a thickness of  $88 \pm 8 \mu\text{m}$  ( $n = 3$ ). There is a variability of approximately  $10 \mu\text{m}$  in the thickness of PLGA shuttles, which is similar to the variation in the PVA-shuttled probes. The variability of the PLGA coating is therefore assumed marginal when compared to the coating approach of the PVA-shuttle.

Electrical impedance characterization was performed next to investigate the influence of the bioresorbable polymers when covering the microelectrodes on the frontside of the probe. The presence of PVA did not seem to interfere with the low impedance of the PEDOT:PSS-coated probes. Before deposition of the polymer on the probes, the average impedance was

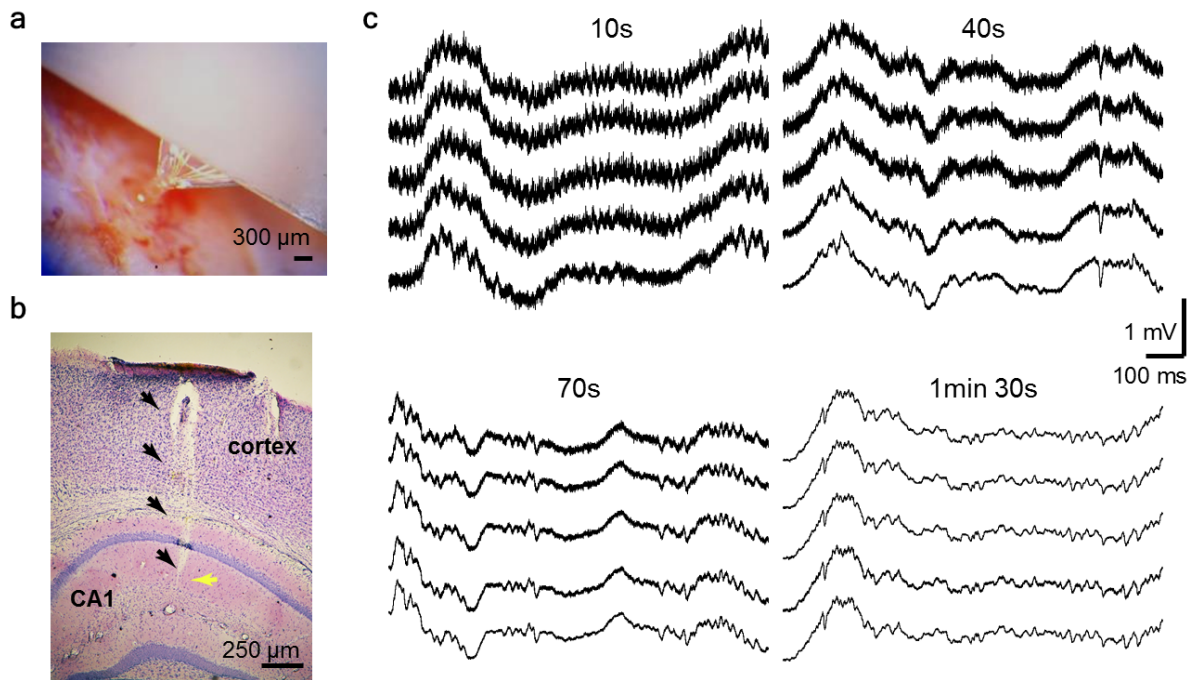


**Figure 4.** *In vivo* characterization of probes. (a) Picture of a probe lowered in the craniotomy performed in an anesthetized mouse. (b) Nissl staining of a  $60\ \mu\text{m}$  brain section showing the trajectory (black arrowheads) of an implanted probe through the cortex and reaching the CA1 region of the hippocampus (yellow arrowhead). Bar =  $250\ \mu\text{m}$ . (c) Recorded data showing LFPs measurements of 5 recording sites of the probe showed in (b). Note the increased quality of the LFP signals recorded with time after the probe insertion, revealing the dissolution of the PVA polymer. The LFP traces are arranged according to the probe sites layout (tip = bottom).

$41.5 \pm 6.4\ \text{k}\Omega$  ( $n = 13$  electrodes) at  $1\ \text{kHz}$  in saline solution. The impedance at that particular frequency was investigated as it is the maximum frequency of electrophysiological signals. Figure 3(e) shows the change in average (red trace), the minimum and maximum values (red dashed lines) of the measured impedance at  $1\ \text{kHz}$  after the addition of the PVA shuttle as a function of immersion time. The impedance was measured every minute from five electrodes ( $n = 5$ ) on five different probes. The graph shows that the impedances decreased to their originally low values (i.e. before deposition) within those 10 min. The min/max became more narrow within that period of time. Of all the 13 investigated electrodes on those five probes, an average impedance of  $73.0 \pm 144.5\ \text{k}\Omega$  ( $n = 13$ ) at  $1\ \text{kHz}$  was observed after more than 10 min of immersion. The slightly larger mean and standard deviation were possibly caused by some remaining PVA residue present at the time of measurement. Overall, the low impedance of PVA-shuttled probes was restored only 10 min after immersion. This corresponds to the dissolution time required to obtain uncovered electrodes.

In contrast, a PVA/PLGA coating covering the electrodes slowed down the restoration of the originally low impedance of the electrodes on the flexible probes. Note that the PLGA coating on the probes for electrical characterization is done on both the front- and backside of the probe to investigate the influence of polymer degradation on electrode impedance. The impedance of three electrodes ( $n = 3$ ) on three different probes was analyzed during immersion of the PVA/PLGA-shuttled probes in saline. The change in average impedance, minimal and maximum are also shown in figure 3(e) (blue traces, from *min* 1 to *min* 10). Unlike observed with PVA shuttles, the impedances of these probes did not decrease to their original

value after 10 min. The coverage of PLGA on the microelectrodes most definitely played a role. The exception to this trend was observed on an electrode of a PVA/PLGA-shuttled probe with PLGA coating on only the backside of the probe (supplementary figure 2). A week after continuous immersion in saline and incubation at  $37\ ^\circ\text{C}$  of the three probes, a gradual decrease in impedance was observed in the electrodes tested (figure 3(e), blue trace from *day* 1 to *day* 7). While an average impedance of  $34.2 \pm 21.7\ \text{k}\Omega$  ( $n = 12$  electrodes) before the deposition of PVA/PLGA was observed, this changed to  $3697.2 \pm 2799.9\ \text{k}\Omega$  after an hour and to  $730.4 \pm 558.7\ \text{k}\Omega$  after a week of immersion (supplementary table 1). At the end of one week, three of the 12 electrodes had an impedance below  $100\ \text{k}\Omega$  (ideal for single unit activity) and nine had an impedance below  $2\ \text{M}\Omega$  (ideal for local field potentials—LFP—recordings).

When further evaluating the change in impedance of the PVA/PLGA coated electrodes for several weeks, the impedance decreased even more (figure 3(e), blue trace from *day* 7 to *week* 4). After four weeks in a saline solution, the average impedance showed to be  $117.9 \pm 130.7\ \text{k}\Omega$  ( $n = 10$  electrodes). At the end, six out of the ten electrodes had an impedance below  $100\ \text{k}\Omega$  and four had an impedance below  $500\ \text{k}\Omega$ . The impedance clearly depended on the degradation of PLGA which was covering the electrodes. PVA/PLGA shuttled probes for *in vivo* recordings were therefore coated with PLGA on the backside of the probe. Nevertheless, it should be noted that electrode impedance is not the only factor determining signal quality [50, 51]. It is more likely that material and biological failures, like material degradation and the occurrence of foreign body response, cause a decrease in signal amplitude [50]. It was however not in the scope of this paper to investigate this.

The fabrication process did yield some bent probes. The cause of bending is most likely due to their sensitivity to humidity at ambient conditions and can generally be prevented by keeping the shuttled-probe inside the PDMS mold until surgery. Bent probes showed poor penetration in the agarose brain models (supplementary figure 3). Due to these penetration challenges, only straight probes were selected for *in vivo* penetration and recording experiments.

PVA/PLGA-shuttled probes were successfully inserted into *in vivo* anaesthetized mice brains ( $n = 8$  probes). An example of a penetrated probe inside the brain is shown in figure 4(a). The trajectory of the probe is shown with a Nissl staining of the brain tissue after fixation of the tissue (figure 4(b)). As shown in the figure, the probe penetrated through the cortex and reached the CA1 region of the hippocampus. A penetration depth of more than 1 millimeter was thus achieved with the bioresorbable shuttle *in vivo*.

Acute *in vivo* measurements were subsequently performed with the inserted probes and resulted in the recording of LFPs (figure 4(c)). Initially, the LFP baseline showed more noise, but tens of seconds after insertion, as the PVA dissolved, this noise reduced to yield an improved signal. This was quantified by computing for each active channel the Root Mean Square (RMS) of the baseline (supplementary figure 4 ( $n = 11$ ) and supplementary figure 5(a) ( $n = 5$ )). A few seconds after probe insertion, LFP traces displayed high RMS values, corresponding to contamination by 50 Hz and high-frequency electrical noise (as revealed by the power spectra of the LFPs, supplementary figure 4(b)). The RMS value of these traces rapidly decreased in time, yielding uncontaminated and high-quality LFPs. After 2 min, high signal-to-noise LFPs were observed at all the recording sites.

In these acute measurements, we demonstrated that very high quality LFP recordings were achieved by using a bioresorbable polymer shuttle to insert flexible probes into the brain. Long-term measurements are needed in order to validate this approach for chronic applications such as brain-machine interfaces. In particular, chronic recordings would be useful to examine changes in impedance and if single action potentials can be recorded since we know the polymer shuttle will continue to degrade *in vivo* past the 10 min presented here. Other valuable future work includes the evaluation of the chronic foreign body response and gliosis, as well as acute tissue damage resulting from different flexible probe insertion methods, such as using microwires [20] or silicon shanks [18] as shuttles, compared to the biodegradable PVA/PLGA shuttles presented here.

## Conclusion

The use of more compliant neural probes requires an additional insertion method to penetrate the brain and place the devices at a precise location. To this end, we present a new bioresorbable polymer shuttle made of the synthetic polymers PVA and PLGA on a flexible parylene-based depth probe. While the rigid PVA shuttle provided the necessary stiffness to penetrate the brain, the added PLGA coating prevented the fast dissolution of PVA to allow insertion several millimeters

deep into the brains of mice. We further showed that the PVA/PLGA shuttles did not affect the electrical properties of the probe, unless PLGA was left covering the microelectrodes on the probes, and demonstrated the recording of high quality LFPs in anaesthetized mice. This work shows great promise to interface the soft brain with compliant depth probes for chronic use and improved biocompatibility. A potential further benefit of this approach would be the delivery of anti-inflammatory drugs through the dissolvable shuttle to minimize inflammation at the brain-electrode interface. In summary, a bilayered, bioresorbable shuttle strategy was successfully used to deliver compliant probes to deep brain tissue sites and to yield high quality electrophysiological recordings *in vivo*.

## Acknowledgments

The authors acknowledge support from the ‘Fondation pour la Recherche Médicale’ under grant agreement DBS20131128446, the Whitaker International Program (AR), the European Union’s Horizon 2020 Research and Innovation Programme under grant agreement No. 732032 (BrainCom), and the King Abdullah University of Science and Technology (KAUST) Office of Sponsored Research (OSR) under award No. OSR-2016-CRG5-3003. In addition, AS, AK and AW acknowledge funding from the European Research Council (ERC) under the European Union’s Horizon 2020 research and innovation programme (grant agreement No 716867) as well as the Excellence Initiative of Aix-Marseille University - A\*MIDEX, a French ‘Investissements d’Avenir’ programme. AK was financed by EC Marie Curie Intra-European Fellowship (Imagine, grant agreement No 625372).

## ORCID iDs

Jolien Pas  <https://orcid.org/0000-0002-8017-7759>

Pascale P Quilichini  <https://orcid.org/0000-0001-9081-8655>

Christophe Bernard  <https://orcid.org/0000-0003-3014-1966>

## References

- [1] Jorfi M, Skousen J L, Weder C and Capadona J R 2015 Progress towards biocompatible intracortical microelectrodes for neural interfacing applications *J. Neural Eng.* **12** 011001
- [2] Chen R, Canales A and Anikeeva P 2017 Neural recording and modulation technologies *Nat. Rev. Mater.* **2** 16093
- [3] Lacour S P, Courtine G and Guck J 2016 Materials and technologies for soft implantable neuroprostheses *Nat. Rev. Mater.* **1** 16063
- [4] Weltman A, Yoo J and Meng E 2016 Flexible, penetrating brain probes enabled by advances in polymer microfabrication *Micromachines* **7** 180
- [5] Rousche P J, Pellinen D S, Pivin D P Jr, Williams J C, Vetter R J and Kipke D R 2001 Flexible polyimide-based intracortical electrode arrays with bioactive capability *IEEE Trans. Biomed. Eng.* **48** 361–71
- [6] Ismailova E et al 2012 Plastic neuronal probes for implantation in cortical and subcortical areas of the rat brain *Int. J. Nanotechnol.* **9** 517–28

- [7] Wester B A, Lee R H and LaPlaca M C 2009 Development and characterization of *in vivo* flexible electrodes compatible with large tissue displacements *J. Neural Eng.* **6** 024002
- [8] Khodagholy D et al 2011 Highly conformable conducting polymer electrodes for *in vivo* recordings *Adv. Mater.* **23** H268–72
- [9] Williamson A et al 2015 Localized neuron stimulation with organic electrochemical transistors on delaminating depth probes *Adv. Mater.* **27** 4405–10
- [10] Minev I R et al 2015 Electronic dura mater for long-term multimodal neural interfaces *Science* **347** 159–63
- [11] Goding J et al 2017 A living electrode construct for incorporation of cells into bionic devices *MRS Commun.* **7** 487–95
- [12] Aregueta-Robles U A, Martens P J, Poole-Warren L A and Green R A 2018 Tailoring 3D hydrogel systems for neuronal encapsulation in living electrodes *J. Polym. Sci. B* **56** 273–87
- [13] Keefer E W, Botterman B R, Romero M I, Rossi A F and Gross G W 2008 Carbon nanotube coating improves neuronal recordings *Nat. Nanotechnol.* **3** 434–9
- [14] Vitale F, Summerson S R, Aazhang B, Kemere C and Pasquali M 2015 Neural stimulation and recording with bidirectional, soft carbon nanotube fiber microelectrodes *ACS Nano* **9** 4465–74
- [15] Kuzum D et al 2014 Transparent and flexible low noise graphene electrodes for simultaneous electrophysiology and neuroimaging *Nat. Commun.* **5** 5259
- [16] Kim D H et al 2009 Silicon electronics on silk as a path to bioresorbable, implantable devices *Appl. Phys. Lett.* **95** 133701
- [17] Hwang S W et al 2012 A physically transient form of silicon electronics with integrated sensors, actuators and power supply *Science* **337** 1640–4
- [18] Felix S et al 2012 Removable silicon insertion stiffeners for neural probes using polyethylene glycol as a biodissolvable adhesive *Conf. Proc. IEEE Eng. Med. Biol. Soc. LLNL-CONF-542891*
- [19] Liu J et al 2015 Syringe-injectable electronics *Nat. Nanotechnol.* **10** 629–36
- [20] Luan L et al 2017 Ultraflexible nanoelectronic probes form reliable, glial scar-free neural integration *Sci. Adv.* **3** e1601966
- [21] Vitale F et al 2018 Fluidic microactuation of flexible electrodes for neural recording *Nano Lett.* **18** 326–35
- [22] Takeuchi S, Ziegler D, Yoshida Y, Mabuchi K and Suzuki T 2005 Parylene flexible neural probes integrated with microfluidic channels *Lab Chip* **5** 519–23
- [23] Lecomte A et al 2015 Silk and PEG as means to stiffen a parylene probe for insertion in the brain: toward a double time-scale tool for local drug delivery *J. Micromech. Microeng.* **25** 125003
- [24] Gilgunn P J et al 2012 An ultra-compliant, scalable neural probe with molded biodissolvable delivery vehicle *2012 IEEE 25th Int. Conf. on Micro Electro Mechanical Systems (MEMS)* pp 56–9
- [25] Xiang Z et al 2014 Ultra-thin flexible polyimide neural probe embedded in a dissolvable maltose-coated microneedle *J. Micromech. Microeng.* **24** 065015
- [26] Agorelius J, Tsanakalis F, Friberg A, Thorbergsson P T, Pettersson L M E and Schouenborg J 2015 An array of highly flexible electrodes with a tailored configuration locked by gelatin during implantation—initial evaluation in cortex cerebri of awake rats *Front. Neurosci.* **9** 331
- [27] Harris J P et al 2011 *In vivo* deployment of mechanically adaptive nanocomposites for intracortical microelectrodes *J. Neural Eng.* **8** 046010
- [28] Lewitus D, Smith K L, Shain W and Kohn J 2011 Ultrafast resorbing polymers for use as carriers for cortical neural probes *Acta Biomater.* **7** 2483–91
- [29] Lo M C et al 2015 Coating flexible probes with an ultra fast degrading polymer to aid in tissue insertion *Biomed. Microdevices* **17** 34
- [30] Khilwani R et al 2016 Ultra-miniature ultra-compliant neural probes with dissolvable delivery needles: design, fabrication and characterization *Biomed. Microdevices* **18** 97
- [31] Ulery B D, Nair L S and Laurencin C T 2011 Biomedical applications of biodegradable polymers *J. Polym. Sci. B* **49** 832–64
- [32] Feig V R, Tran H and Bao Z 2018 Biodegradable polymeric materials in degradable electronic devices *ACS Cent. Sci.* **4** 337–48
- [33] Wang Y et al 2008 *In vivo* degradation of three-dimensional silk fibroin scaffolds *Biomaterials* **29** 3415–28
- [34] Lo M et al 2018 Evaluating the *in vivo* glial response to miniaturized parylene cortical probes coated with an ultra-fast degrading polymer to aid insertion *J. Neural Eng.* **15** 036002
- [35] Muppalaneni S 2013 Polyvinyl alcohol in medicine and pharmacy: a perspective *J. Dev. Drugs* **2** 112
- [36] Makadia H K and Siegel S J 2011 Poly lactic-co-glycolic acid (PLGA) as biodegradable controlled drug delivery carrier *Polymers* **3** 1377–97
- [37] Yang D, Li Y and Nie J 2007 Preparation of gelatin/PVA nanofibers and their potential application in controlled release of drugs *Carbohydr. Polym.* **69** 538–43
- [38] Wang X, Yucel T, Lu Q, Hu X and Kaplan D L 2010 Silk nanospheres and microspheres from silk/pva blend films for drug delivery *Biomaterials* **31** 1025–35
- [39] Li X, Kanjwal M A, Lin L and Chronakis I S 2013 Electrospun polyvinyl-alcohol nanofibers as oral fast-dissolving delivery system of caffeine and riboflavin *Colloids Surf. B* **103** 182–8
- [40] Sequeira J A D, Santos A C, Serra J, Veiga F and Ribeiro A J 2018 Poly(lactic-co-glycolic acid) (PLGA) matrix implants *Nanostructures for the Engineering of Cells, Tissues and Organs* (New York: Elsevier) pp 375–402
- [41] Steriade M, Timofeev I and Grenier F 2001 Natural waking and sleep states: a view from inside neocortical neurons *J. Neurophysiol.* **85** 1969–85
- [42] Mitra P P and Pesaran B 1999 Analysis of dynamic brain imaging data *Biophys. J.* **76** 691–708
- [43] Quilichini P, Sirota A and Buzsaki G 2010 Intrinsic circuit organization and theta-gamma oscillation dynamics in the entorhinal cortex of the rat *J. Neurosci.* **30** 11128–42
- [44] Martin D and Malliaras G 2016 Interfacing electronic and ionic charge transport in bioelectronics *ChemElectroChem* **3** 686–8
- [45] Khodagholy D et al 2014 NeuroGrid: recording action potentials from the surface of the brain *Nat. Neurosci.* **18** 310–5
- [46] Kamoun E A, Chen X, Mohy Eldin M S and Kenawy E-R S 2015 Crosslinked poly(vinyl alcohol) hydrogels for wound dressing applications: a review of remarkably blended polymers *Arab. J. Chem.* **8** 1–14
- [47] Nair L S and Laurencin C T 2007 Biodegradable polymers as biomaterials *Prog. Polym. Sci.* **32** 8–9
- [48] Amann L C, Gandall M J, Lin R, Liang Y and Siegel S J 2010 *In vitro*–*in vivo* correlations of scalable PLGA-risperidone implants for the treatment of schizophrenia *Pharm. Res.* **27** 1730–7
- [49] Ramachandran R et al 2017 Theranostic 3-dimensional nano brain-implant for prolonged and localized treatment of recurrent glioma *Sci. Rep.* **7** 43271
- [50] Barrese J C et al 2013 Failure mode analysis of silicon-based intracortical microelectrode arrays in non-human primates *J. Neural Eng.* **10** 066014
- [51] Malaga K A et al 2016 Data-driven model comparing the effects of glial scarring and interface interactions on chronic neural recordings in non-human primates *J. Neural Eng.* **13** 016010